

# Preparation, Characterization, and Property Testing of Condensation-Type Silicone/Montmorillonite Nanocomposites

A. Voulomenou, P. A. Tarantili

*Polymer Technology Laboratory, School of Chemical Engineering, National Technical University of Athens, Heroon Polytechniou 9, Zographou, Athens GR 15780, Greece*

Received 29 May 2009; accepted 21 October 2009

DOI 10.1002/app.31648

Published online 29 June 2010 in Wiley InterScience (www.interscience.wiley.com).

**ABSTRACT:** Nanocomposites (NCs) of silicone rubber and organically modified montmorillonite (OMMT) nanoparticles were prepared and characterized. It was shown that OMMT loadings of 2 and 3.5 parts per hundred resin/filler per weight (phr) produced exfoliation or delamination hybrids, whereas at a concentration of 5 phr, the filler seemed to retain its original crystallographic morphology, and the system shifted to an ordinary reinforced elastomer. Fourier transform infrared analysis, differential scanning calorimetry, and thermogravimetric analysis testing were performed for characterization and showed no effect of the nanofiller on the structural parameters of the composites, with the exception of a reduction in the crystallinity. Dynamic mechanical analysis revealed an increase in the glass-transition temperature ( $T_g$ ) at OMMT concentrations of 2 and 3.5

phr, whereas at 5 phr,  $T_g$  dropped again. Finally, mechanical testing showed an improvement in the tensile strength and stiffness, whereas improved solvent resistance was recorded by swelling experiments in toluene. This experimental study allowed us to explore the range where the OMMT filler produced NCs with silicone elastomers and, furthermore, showed that the incorporation of OMMT into silicone rubber did not introduce any chemical changes but increased the density of crosslinks; this led to a loss of crystallinity, an increase in  $T_g$ , and a significant improvement in the tensile properties. © 2010 Wiley Periodicals, Inc. *J Appl Polym Sci* 118: 2521–2529, 2010

**Key words:** mechanical properties; nanocomposites; organoclay; polysiloxanes; thermal properties

## INTRODUCTION

Polydimethylsiloxane (PDMS) is probably the most important and most useful high-performance elastomer but only when its inherent mechanical weakness is overcome by reinforcement with some particulate fillers, usually silica and titania.<sup>1</sup> Nanoparticles often strongly influence the properties of composites at very low volume fractions. This is mainly a result of the small fraction of polymer matrix near their surfaces in an interphase of different properties and of the consequent change in morphology. As a result, the desired properties are usually reached at a low filler volume fraction, which allows the nanocomposite (NC) to retain the homogeneity and low density of the polymer. Because of the high price of aerosilica and its easy agglomeration, researchers have focused on the development of other reinforcing fillers, such as montmorillonite (MMT), in an attempt to replace aerosilica.<sup>2</sup> Polymer/clay NCs

have recently attracted a great deal of interest because of their unique properties, such as their enhanced mechanical properties, increased thermal stability, improved gas barrier properties, and reduced flammability. On the basis of the arrangement of the silicate layers in a polymer matrix, two types of morphology can be achieved in NCs: intercalated or exfoliated.<sup>3</sup> More specifically, in intercalated NCs, the polymer chains penetrate into the space between the parallel planes of MMT, whereas exfoliated systems are produced via the complete separation and dispersion of those planar nanoparticles within the silicone matrix. The latter procedure has been well recognized as leading to better morphology for higher performance with lower clay loadings but is often difficult to achieve. Because of its hydrophilic nature, clay is generally modified by quaternary ammonium surfactants to increase the intergallery spacing and to achieve enough hydrophobicity to make it miscible with the polymer matrix.

Two types of surfactants are currently used: the first type includes those reactive surfactants that contain functional groups, such as hydroxyl groups and double bonds, that can react with the polymer matrix to form strong linkages between the matrix and clay. The other type of modification uses

Correspondence to: P. A. Tarantili (taran@chemeng.ntua.gr).

surfactants that contain molecular units similar to those of the polymer matrix.<sup>3</sup>

The modified or organophilic clay can be then dispersed into the appropriate polymer matrix by a variety of methods, which can be divided into three categories: (1) intercalation of prepolymer or polymer from solution, (2) melt intercalation, and (3) *in situ* intercalative polymerization.<sup>3</sup>

Burnside and Giannelis<sup>4</sup> reported on PDMS/organically modified montmorillonite (OMMT) NCs with the use of melt intercalation. The organosilicate was prepared by the ion exchange of Na<sup>+</sup>-MMT with dimethyl ditallow ammonium bromide. The prepared NCs exhibited decreased solvent uptake and increased thermal stability.

In another study, organosilicate was also prepared by the ion exchange of Na<sup>+</sup>-MMT with hexadecyltrimethylammonium bromide, and silicone rubber/OMMT hybrids were prepared by simple mechanical mixing.<sup>5</sup> The mechanical properties and thermal stability of the hybrids were very close to those of aerosilica-filled silicone rubber.

LeBaron and Pinnavaia<sup>6</sup> used a synthetic fluorohectorite clay, in which the exchange cations were replaced by hexadecyltrimethylammonium ions. Their scope was to prepare intercalated structures with linear PDMS molecules containing terminal hydroxyl groups. The nanolayer-reinforced polymer exhibited substantially improved tensile properties, resistance to swelling by organic solvents, and reduced structural damage caused by internal strain induced by allowing the solvent to evaporate from the swollen polymer network. However, a small reduction in oxygen permeability was observed in these NCs.

A two-step process was reported for the preparation of the exfoliated/intercalated polymer/MMT NCs, which included the preparation of an MMT solution via the *in situ* polymerization of dimethyldichlorosilane inside the galleries of layered silicate hosts and then, after the separation of most of the PDMS, the blending of the treated MMT solution with several polymers.<sup>7</sup>

A new strategy to prepare disorderly PDMS NCs was developed by Ma et al.,<sup>8</sup> in which a soft siloxane surfactant was adopted to modify the clay. The modified clay slurry was then mixed with silicone rubber by hand, and exfoliation was achieved; this was confirmed by transmission electron microscopy and X-ray diffraction (XRD) analysis.

A novel kind of OMMT was successfully prepared by Wang et al.<sup>2</sup> with *N,N*-di(2-hydroxyethyl)-*N*-dodecyl-*N*-methylammonium chloride as an intercalation agent. Exfoliated NCs were prepared with addition-type silicone rubber via solution intercalation. More specifically, the authors treated MMT with a solution of the previous quaternary ammonium salt and claimed to have so efficiently opened its struc-

ture that the subsequent addition of liquid silicone elastomer resulted in the exfoliation of the MMT planes. The enhanced mechanical and physical properties demonstrated the efficient reinforcement and thermal stability properties of OMMT.

To overcome difficulties during the preparation of high-temperature-vulcanized silicone rubber (HTV-SR) NCs, a master batch of the previously mentioned modified montmorillonite (OMMT-MB) was prepared by solution intercalation by Wang and Chen.<sup>9</sup> HTV-SR/OMMT-MB-20% NCs demonstrated enhanced tensile and thermal properties in comparison with HTV-SR/OMMT-20%.

An alternative technique was proposed by Horsch et al.,<sup>10</sup> who used supercritical carbon dioxide to delaminate dry clays and found that the extent of dispersion was dependent on the CO<sub>2</sub>-philicity of the nanoclay. In addition, natural clay was partially dispersed with supercritical carbon dioxide with a CO<sub>2</sub>-philic PDMS matrix.

From the study of a multisystem, it has been shown that in NCs based on silanol-terminated PDMS and alkylammonium modified layered-silicate fillers, there are two factors controlling silicate dispersion: (1) the presence of an appropriate number of long ammonium-bound alkyl chains and (2) the presence of an appropriate number of polar functional groups. Therefore, dispersion is not an issue of molecular weight or viscosity-induced differences in processing but of silanol end-group concentration.<sup>11</sup>

In this study, OMMT composites with high-viscosity hydroxyl-terminated PDMS were prepared by sonication at room temperature. The composites were characterized with XRD, infrared spectroscopy [Fourier transform infrared (FTIR)-attenuated total reflection (ATR)], thermogravimetric analysis (TGA), and differential scanning calorimetry (DSC). In addition, the dynamic mechanical properties, tensile properties, and solvent uptake were studied.

## EXPERIMENTAL

### Materials

Hydroxyl-terminated PDMS, grade Silopren C70 (Momentive, Inc., Albany, NY), was vulcanized at room temperature, with 10-phr tetrapropoxysilane (Aldrich, Germany) as a crosslinker and 0.1-phr dibutyl tin dilaurate (Aldrich) as a catalyst. Commercial MMT clay under the trade name Cloisite 20A, supplied by Southern Clay Products, Inc., (Gonzales, TX) was used. The main characteristics of this clay are presented in Table I.

### Preparation of the NCs

Efficient dispersion of the nanoparticles was achieved by sonication with an ultrasound probe of the PDMS

**TABLE I**  
Main Characteristics of the Nanoclay Used in This Study

Cloisite 20A	
Organic modifier	Dimethyl dihydrogenated tallow quaternary ammonium: $\begin{array}{c} \text{CH}_3 \\   \\ \text{CH}_3 - \text{N}^+ - \text{HT} \\   \\ \text{HT} \end{array}$
	where HT is hydrogenated tallow (~ 65% C18, ~ 30% C16, and ~ 5% C14)
Modifier concentration	95 mequiv/100 g of clay
Weight loss in ignition	38%

and an appropriate amount of clay for 8 min at room temperature. The crosslinking agents were then added and dispersed into the mixture, and the samples were cast into molds and cured at room temperature for 12 h.

### XRD

XRD of the clay and NCs was performed to detect the evolution of the clay  $d_{001}$  reflection. A Siemens 5000 apparatus (35 kV, 25 mA) was used with Cu  $K\alpha$  X-ray radiation with a wavelength of 0.154 nm. The diffractograms were scanned in the  $2\theta$  range from 2 to  $10^\circ$  at a rate of  $2^\circ/\text{min}$ .

### ATR-FTIR spectroscopy

For the determination of changes in the chemical structure of the OMMT/PDMS composites, ATR measurements were performed with a Nicolet (Madison, WI) FTIR spectrometer (model Magna IR 750, deuterated triglycine sulfate (DTGS) detector, Nichrome source, beam splitter; KBr). A total of 100 scans were applied with a resolution up to  $4\text{ cm}^{-1}$ . Spectra were obtained in the ATR mode with a standard ZnSe  $45^\circ$  flat plate contact sampler (12 reflections, Spectra-Tech), on which samples of PDMS were placed (100  $\mu\text{L}$ ). The obtained spectroscopic data were treated with standard software (OMNIC 3.1, Nicolet).

All spectra were smoothed with the automatic smooth function of the software, which used the Savitsky–Golay algorithm (5-point moving second-degree polynomial). After this procedure, the baseline was corrected with the automatic baseline-correction function.

### TGA

Thermogravimetric tests in the OMMT/PDMS NCs were performed with a Mettler Toledo (Schwerzenbach, Switzerland) thermogravimetric analyzer (model TGA-SDTA 851E). The analysis was run with samples of 10 mg at a heating rate of  $10^\circ\text{C}/\text{min}$  from 25 to  $700^\circ\text{C}$  in a nitrogen atmosphere.

### DSC

DSC measurements were performed in a PerkinElmer (Waltham, MA) model Pyris 6 differential scanning calorimeter with pure indium as a calibration standard. Samples of approximately 10 mg were accurately weighed in an analytical balance and encapsulated in aluminum pans. All runs were conducted under a nitrogen flow of  $20\text{ cm}^3/\text{min}$  to limit thermooxidative degradation. The samples were cooled with liquid nitrogen from 30 to  $-120^\circ\text{C}$  at a rate of  $10^\circ\text{C}/\text{min}$ ; we kept them at this temperature for 3 min to erase previous thermal history. After this treatment, the samples were heated from  $-120$  to  $30^\circ\text{C}$  at  $10^\circ\text{C}/\text{min}$ .

### Dynamic mechanical analysis (DMA)

DMA experiments were performed in a PerkinElmer Analyzer (Diamond DMA) in tension mode over temperatures ranging from  $-150$  to  $50^\circ\text{C}$  at  $1^\circ\text{C}/\text{min}$ .

### Tensile testing

Tensile tests were carried out according to the ASTM D 412 specification in an Instron (Bucks, UK) tensometer (model 4466), equipped with a load cell with a maximum capacity of 10 kN, operating at grip separation speed of 100 mm/min. All measurements were run at  $25^\circ\text{C}$ .

### Swelling experiments

The solvent uptakes of the immersed PDMS NC samples were also measured at  $25^\circ\text{C}$ . Preweighed samples were immersed in toluene, and at different time intervals, the swollen samples were rapidly blotted and reweighed to minimize the evaporation of toluene. Reweighing continued for a few days, and the final weight of the swollen sample was recorded at the equilibrium state.

## RESULTS AND DISCUSSION

### Preparation of the OMMT/PDMS composites

The incorporation of OMMT in PDMS resulted in an increase in the viscosity and extended the

**TABLE II**  
**Vulcanization Characteristics of the Cloisite 20A (OMMT)/PDMS Systems**

OMMT/PDMS (phr)	Viscosity (cP)	Vulcanization time (h)
0	48,800	1.5
2	56,400	2.0
3.5	61,200	2.5

vulcanization time, as shown by the data in Table II. The increased viscosity did not play a critical role in the dispersion capability of the filler particles, which was mainly affected by the silanol end-group concentration.<sup>11</sup> On the other hand, an increase in the system viscosity was responsible for higher shear stresses during the mixing procedure and might have been beneficial for better filler dispersion. However, the relatively high molecular weight of PDMS used in this study reflected the long polymer chain and, furthermore, a reduced end-group concentration, which confined the dispersion ability. On the other hand, the clay nanoparticles were characterized by a high aspect ratio, and their possible interactions with the crosslinker or the silicone elastomer might have been a reason for the increase in the vulcanization time of the system.

So far, interesting results regarding the effect of nanoparticles on the vulcanization process of elastomers have been reported. Yang et al.<sup>12</sup> claimed that in the rubber vulcanizing crosslinking process, OMMT could perform as active sites to increase the crosslinking degree and lead to netlike structures of increased density.

Chemical interactions between the alkoxy silicane catalyst of the hydroxyl-containing PDMS and the intercalation agent of MMT [di(2-oxyethyl)-12-alkane-3-methyl amine chloride] was mentioned to have an important effect on the intercalation and exfoliation of the organoclay.<sup>13</sup>

Studies of the vulcanization kinetics of natural rubber–organoclay NCs by López-Manchado et al.<sup>14</sup> showed that the modified clay behaved as an effective vulcanizing agent and had an accelerating effect on the vulcanization reaction of the elastomer. Moreover, in the presence of organoclay, a dramatic increase in the torque value was observed because of the formation of a higher crosslink density, which could be attributed to the confinement of the elastomer chains within the silicate galleries. It is obvious that such a mechanism is expected to induce better interactions between the filler and the rubber.

In a recent study,<sup>15</sup> the tube model was applied as a means of evaluating the influence of inorganic nanoparticles on the crosslinking mechanism of elastomers. The results showed that a highly ordered structure with a huge amount of entanglements, wherein the polymer was nanoscopically confined,

was formed by the addition of nanoparticles. These physical links exhibited freedom of movement under stretching but in a lower volume because of the confinement.

## XRD

XRD analysis was conducted for the assessment of the status of clay dispersion within the polymer matrix. It is well known that with Bragg's rule (i.e.,  $2d \sin \theta = n\lambda$ ; where  $d$  is the (.001) basal spacing of the clay,  $\theta$  is the angle of reflection,  $n$  is an integer, and  $\lambda$  is the wavelength = 0.1540569 nm with Cu-ka radiation), the basal spacing for clay layers can be calculated.

The XRD patterns for Cloisite 20A, the sample of PDMS with 2-phr Cloisite 20A, and composites prepared with different mixing conditions are shown in Figure 1.

Cloisite 20A was characterized by relatively high content of organic modifier (Table I) and high intergallery spacing, which facilitated its intercalation in the PDMS matrix. In addition, it was possible that the hydrogenated tallow incorporated into Cloisite 20A enhanced the compatibility of the nanofiller with the silicone rubber system.

However, it was reported that in real NCs, complete exfoliation cannot be achieved, but most materials show a combination of various dispersion states, either as a result of inhomogeneous mixing or, simply, because of the fact that the transition from intercalated structure to an exfoliated cannot be clearly defined and numerous intermediate states may exist.<sup>16</sup>

A series of XRD patterns of PDMS composites containing various OMMT loadings are shown in Figure 2. The featureless patterns for loadings of 2- and 3.5-phr OMMT suggest that exfoliation or delamination hybrids were formed. For clay contents up to 5 phr, the presence of the reflection peak became obvious, which indicated that filler particles in that concentration remained intact to some

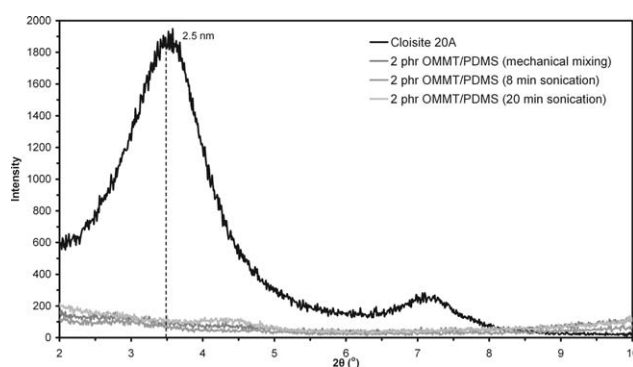


**Figure 1** XRD patterns of Cloisite 20A and the 2-phr Cloisite 20A/PDMS NCs.

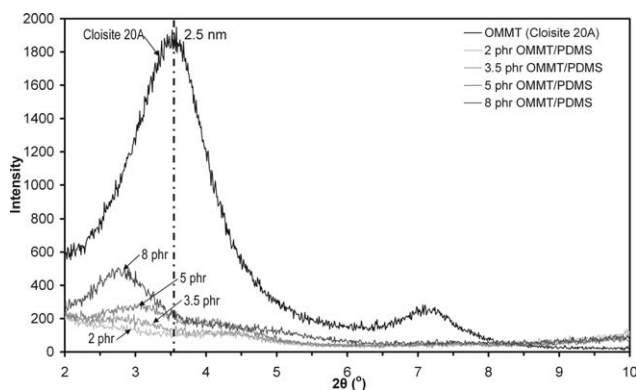


**Figure 2** XRD patterns of Cloisite 20A and its composites.

significant extent, and therefore, the system corresponded to a usual reinforced elastomer rather than an NC.

### ATR-FTIR spectroscopy

The IR spectra of the silicone elastomer, unfilled and filled, with different loadings of OMMT are presented in Figure 3.

The  $3630\text{-cm}^{-1}$  peak, corresponding to stretching of  $\text{—OH}$ , was attributed to the physical and chemical effects of water within the MMT. The peak at  $1010\text{ cm}^{-1}$  was associated with the stretching vibration of  $\text{Si—O}$  bond in the MMT structure. The peaks at  $2800\text{—}3000$  and  $1467\text{ cm}^{-1}$  corresponded to the  $\text{C—H}$  stretching and bending absorptions in the organic intercalation agent. Furthermore, PDMS exhibited a

series of characteristic IR bands. Among the most intense were those associated with  $\text{—CH}_3$  rocking and  $\equiv\text{Si—CH}_3$  stretching ( $785\text{ cm}^{-1}$ ),  $\equiv\text{Si—OH}$  stretching ( $864\text{ cm}^{-1}$ ), asymmetric  $\equiv\text{Si—O—Si}\equiv$  stretching in  $[-(\text{CH}_2)_2\text{Si—O—}]_x$  ( $1077\text{ cm}^{-1}$ ), symmetric  $\text{—CH}_3$  deformations in  $\equiv\text{Si—CH}_3$  ( $1258\text{ cm}^{-1}$ ), and asymmetric  $\text{—CH}_3$  stretching in  $\equiv\text{Si—CH}_3$  ( $2962\text{ cm}^{-1}$ ).

The positions of the peaks for distinctive functional groups were almost identical in the pure PDMS and OMMT/PDMS composites. This means that the segmented structure of PDMS was not affected by the presence of OMMT.

Wang et al.<sup>13</sup> found that with increasing OMMT amount added to room-temperature-vulcanized silicone rubber (RTV-SR), the intensity of the absorption peaks at  $1070\text{—}1090$  and  $800\text{ cm}^{-1}$  appeared to decrease in comparison with that of those of pure silicone. They explained this behavior by a chemical reaction of the alkoxy silane catalyst, not only with the hydroxyl-containing base rubber but also with the hydroxyl groups of the organic modifier of MMT. These interactions were competitive to  $\text{Si—O—Si}$  group formation, that is, a chemical reaction taking place freely in the pure RTV-SR system.

### TGA

As shown in Table III and Figure 4, the OMMT/PDMS NCs presented a lower initial temperature of thermal degradation in comparison with PDMS, probably because of the degradation of short molecular chains of intercalated agents. The higher amounts of char residue were attributed to the enhancement of the thermal stability of these

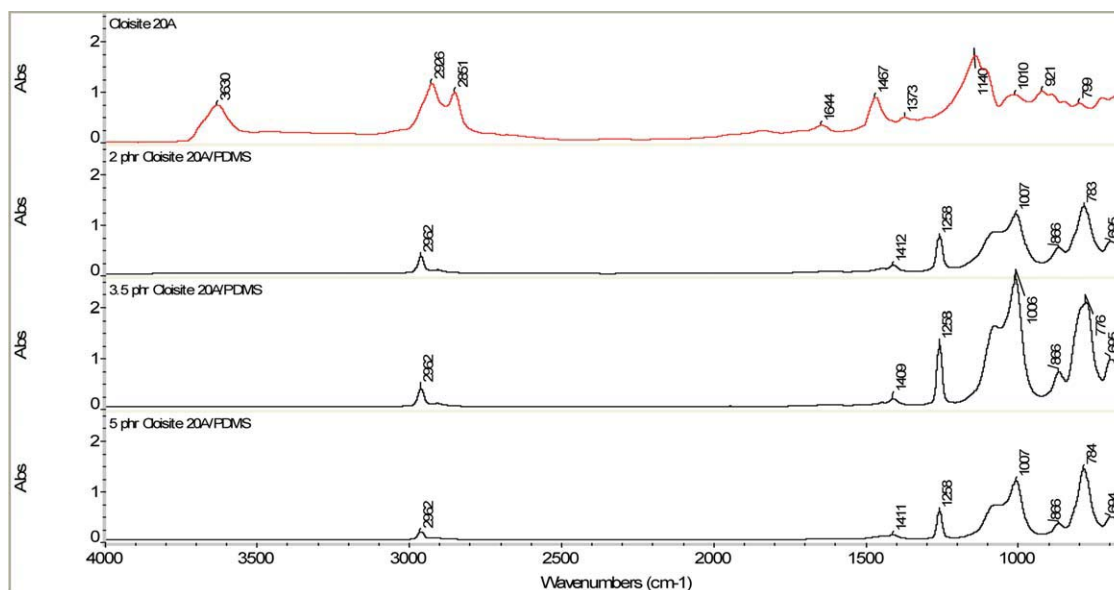


**Figure 3** ATR-FTIR spectra of the OMMT/PDMS composites as a function of the OMMT content. [Color figure can be viewed in the online issue, which is available at [www.interscience.wiley.com](http://www.interscience.wiley.com).]

**TABLE III**  
TGA Data of the OMMT/PDMS Composites

OMMT content in PDMS (phr)	Onset temperature of thermal degradation (°C)	Temperature of maximum thermal degradation rate (°C)	Char residue (%)
0	492.39	563.17	3.15
2	501.36	554.83	4.76
3.5	491.06	546.00	7.23
5	472.02	535.17	8.57

products because of the nanosilicate layers produced during the heating process.<sup>9</sup>

An improvement in the thermal stability of OMMT/hydroxyl-terminated PDMS hybrids, very close to those of aerosilica-filled silicone rubber, was also reported by Wang et al.<sup>5</sup> An increase in the char residue and promising flame retardant properties were determined when methyl vinyl silicone rubber NCs containing 1 wt % MMT were tested by TGA.<sup>12</sup>

Wang et al.<sup>2</sup> observed a decrease in the char residue with increasing amount of OMMT in addition-type silicone rubber composites, whereas the initial and center temperatures of the thermal degradation of these samples showed first an increase and then a decrease. Similar behavior was reported for hydroxyl-containing silicone rubber composites, which are known to vulcanize via the condensation of hydroxyl end groups.<sup>13</sup> It was concluded that there were two factors influencing the thermal stability of the composites: (1) the incorporation of efficiently dispersed OMMT, which could prevent heat transport and thus improve the thermal stability of the composites, and (2) the OMMT contained some molecules that could be released even at low temperatures, and some of them certainly could impair the thermal stability of the composites. Finally, Kim et al.<sup>17</sup> found that the activation energy of the thermal degradation increased significantly by the introduction of Cloisite 30B in hydroxyl-terminated PDMS.

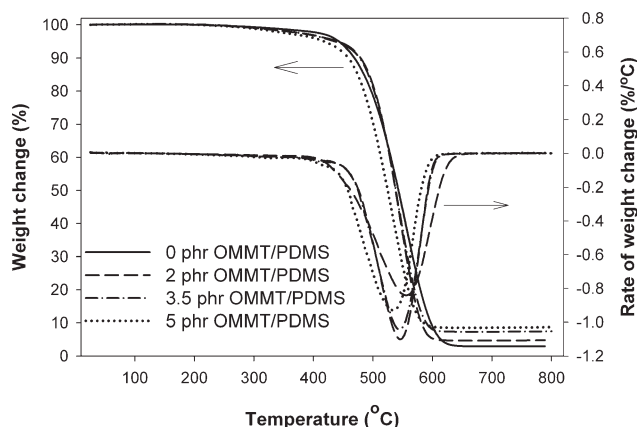


**Figure 4** TGA curves of the OMMT/PDMS composites.

**TABLE IV**  
DSC Analysis Data of the OMMT/PDMS Composites

OMMT content in PDMS (phr)	$T_m$ (°C)	$\Delta H_c$ (J/g)	$T_c$ (°C)	$\chi_c$ (%)
0	-47.68	27.06	-77.05	69.32
2	-47.01	24.13	-74.91	67.36
3.5	-47.35	23.57	-74.10	64.99
5	-47.34	22.57	-74.34	63.02

Taking into consideration the previously presented experimental evidence as derived from the related literature, we concluded that the increase in char residue observed in the OMMT-containing NC samples could have been a result of the efficient filler dispersion and the formation of nanosilicate layers during the heat treatment of the samples. These layers could evenly dissipate the heat within the sample under testing and improve its thermal stability, at least in terms of the ultimate loss of material.

## DSC

The thermal transitions were determined with the appropriate calorimeter (DSC) in an atmosphere of flowing nitrogen and capable of being cooled with liquid nitrogen. The obtained results are presented in Table IV and show that pure PDMS and Cloisite 20A NCs displayed a melting point near  $-47^\circ\text{C}$ . The degree of crystallinity ( $\chi_c$ ) of the polymer in each sample was determined from the enthalpy of crystallization ( $\Delta H_c$ ) as the ratio of its value to the enthalpy corresponding to the pure polymer, that is,  $\chi_c = \Delta H_c / \Delta H_{100\%}$ , where  $\Delta H_{100\%}$  is the enthalpy of fusion of PDMS, which was taken as 37.43 J/g. During cooling, the PDMS crystallized at  $-77^\circ\text{C}$ . The cold crystallization temperature for the PDMS NCs showed an increase of about  $2\text{--}3^\circ\text{C}$ , which was accompanied by a slight decrease in the heat of crystallization.

As shown in Table IV and Figure 5, the incorporation of OMMT did not have any obvious effect on

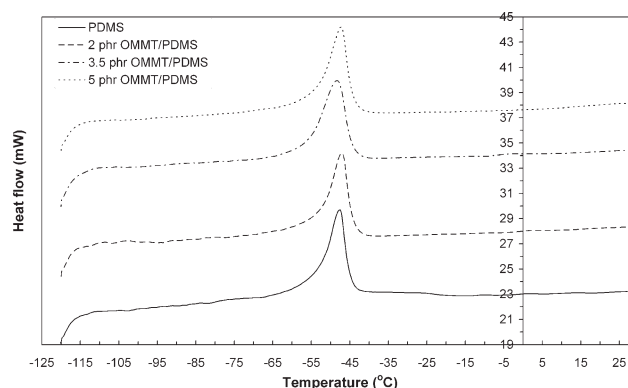


**Figure 5** DSC curves of the OMMT/PDMS composites.

the melting temperature ( $T_m$ ), which remained almost constant, but the heat of fusion decreased.

Similar results, with regard to the effect of the amount of OMMT filler incorporated into the silicone rubber on its melting point, were reported by Wang et al.<sup>13</sup> According to these authors, the melting point could be affected by at least three factors: (1) the reinforcing effect of the OMMT layers, together with the intercalation polymer chains, which thus gave rise to an increase in  $T_m$ ; (2) the dispersed silicate layers in the matrix, which might have served as nucleation seeds and induced some additional crystallinity within the silicone matrix, which further restricted the chain motion; and (3) incomplete curing due to reactions of silicone rubber components, not only with polysiloxane but also with other chemicals present in the system, such as the intercalation agent. According to the previous discussion, it is obvious that within the experimental setup of our study, the dispersed OMMT nanoparticles did not seem to contribute to the overall crystallinity of the NC systems because the parameters  $\Delta H_c$  and  $\chi_c$  tended to decrease, whereas the melting point of the composite seemed to remain constant with filler concentration.

Very interestingly, Burnside and Giannelis<sup>18</sup> reported a fairly constant crystallization temperature ( $T_c$ ) for PDMS NCs, but their  $\Delta H_c$  dramatically decreased. In addition, they found that the melting transitions remain unchanged, but the heat of fusion decreased, which was in agreement with the results obtained in this study.

## DMA

The effect of the incorporation of organically modified layered silicate particles on the viscoelastic properties of the vulcanized PDMS was studied by

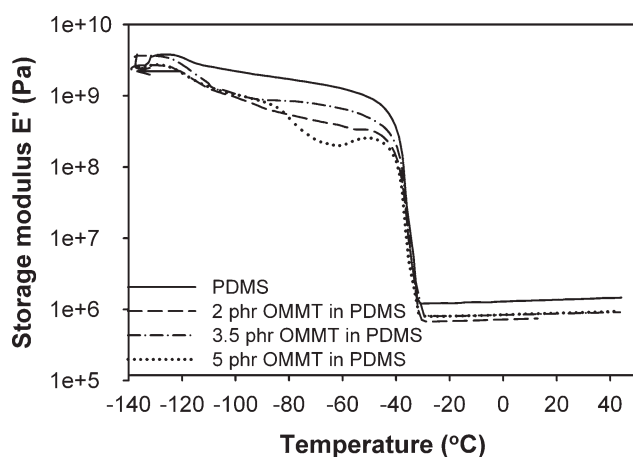


**Figure 6** Temperature dependence of the elastic modulus for PDMS and the OMMT/PDMS composites at a frequency of 1 Hz.

**TABLE V**  
DMA Data of the OMMT/PDMS Composites  
Derived from the  $\tan \delta$ /Temperature Graph  
at a Frequency of 1 Hz

OMMT content in PDMS (phr)	$T_m$ (°C)	$T_g$ (°C)
0	-38.92	-120.32
2	-40.43	-115.84
3.5	-39.68	-106.27
5	-40.02	-116.76

DMA. This method is recommended for the study of the dynamic properties of neat PDMS and OMMT/PDMS composites over a wide temperature range (-150 to 50°C). The storage modulus as a function of temperature is shown in Figure 6. The addition of OMMT in PDMS did not essentially affect the properties of the rubber. However, a shift in the glass-transition temperature ( $T_g$ ) to higher temperatures, as compared to that of pure PDMS, is shown in Table V for the OMMT-based NCs.

Similar behavior was recorded by Carretero-González et al.,<sup>19</sup> who studied NC systems of natural rubber reinforced with nanoclays. It is reasonable that the observed increase of  $T_g$  suggests a strong interaction between the filler and matrix, which resulted in restricted mobility of the polymer chains in the presence of clay nanoparticles. In our case, where the experimental evidence showed, thus far, an efficient filler dispersion in the NC samples with no essential chemical interaction between the OMMT particles and silicone matrix nor extra crystallinity formation, we concluded that filler nanoparticles contributed to the increase in the density of crosslinks. This was observed for filler concentrations of 2 and 3.5 phr; this was in agreement with the XRD analysis data, which showed that exfoliation or delamination hybrids were formed at those OMMT loadings. On the other hand, for an OMMT concentration of 5 phr,  $T_g$  dropped again, which might have been the result of the aforementioned structure of the reinforced silicone elastomer.

Also, the  $T_m$  values of the pure and reinforced silicone determined by DMA were essentially higher (ca. 7°C) than those recorded by the DSC method. However, in both cases of analysis,  $T_m$  seemed to remain unaffected by the concentration of OMMT filler incorporated into the silicone rubber matrix.

## Tensile testing

Mechanical testing revealed that the incorporation of OMMT increased the tensile strength (48%) and modulus of elasticity (28%) of silicon rubber, and these changes were accompanied by an increase in the elongation at break (Table VI).

TABLE VI  
Tensile Test Results of the OMMT/PDMS Composites

OMMT content in PDMS (phr)	Tensile strength (MPa)	Modulus of elasticity (MPa)	Strain at break (%)
0	0.338 ± 0.047	0.811 ± 0.057	85.29 ± 7.174
2	0.395 ± 0.016	0.825 ± 0.240	114.40 ± 8.150
3.5	0.368 ± 0.039	0.896 ± 0.181	95.80 ± 9.474
5	0.396 ± 0.054	0.854 ± 0.056	140.20 ± 10.700

Ma et al.<sup>8</sup> reported an increase of 105% in the tensile strength of PDMS exfoliated NCs reinforced with 2 wt % clay modified with a soft siloxane surfactant. A synergistic reinforcing effect was observed for systems based on methyl vinyl silicone rubber containing SiO<sub>2</sub>/OMMT as a filler.<sup>12</sup>

These results were in agreement with the increase of  $T_g$  observed during the DMA tests. A good dispersion of the OMMT into the silicone matrix and some possible interactions of filler particles with silicone chains, which might have created additional crosslinks, resulted in final products with increased mechanical strength and stiffness.

### Swelling

Swelling experiments with specimens from the reinforced silicone matrix (PDMS NCs) immersed in toluene exhibited a slight decrease in solvent uptake compared to that corresponding to the unfilled PDMS matrix, as shown in Figure 7. Toluene uptake was controlled by Fickian diffusion for the first 8 h of the experiment, and then, a plateau was observed. The PDMS NCs studied in this work did not present significantly improved solvent uptake resistance, as was expected from the data of the related literature.<sup>4,18,20</sup>

Two mechanisms may have controlled the toluene diffusion in the PDMS matrix:

1. The increase in the tortuosity path due to the presence of the dispersed nanoparticles in the PDMS matrix.
2. The network density of the crosslinked elastomer.

As already stated for the NC systems studied in this work, the increased surface area of the nanoparticles might have promoted some interactions with the silicone matrix and, therefore, led to the formation of additional crosslinks, which could have led to increased network density in the final product. This corresponded to lower solvent uptake and swelling of the filled NC.

Similarly, Burnside and Giannelis<sup>4</sup> observed a significant decrease in the solvent uptake of PDMS–silicate dispersed NCs, as compared to intercalated or immiscible hybrids, even at filler concentrations

of 1 v/v %. They reported that strongly interacting fillers reduced swelling because of the formation of bound polymer in close proximity to the filler, which was either physisorbed or chemisorbed and, therefore, restricted swelling. In a recent study, these researchers found that the swelling behavior mirrored the amount of bound polymer in the NC, and they concluded that the swelling behavior arose from the nanostructure rather than from the increased crosslinks density determined in the network.<sup>18</sup>

Takeuchi and Cohen<sup>20</sup> studied MMT/PDMS NCs and observed that an improvement in the properties of the PDMS network, in terms of higher modulus and lower swelling in good solvents, was obtained only for nonoptimal networks formed with hydroxyl-terminated precursor chains but not with vinyl-terminated chains. Their results indicate that the reinforcement of these elastomers was due to the anchoring of the hydroxyl end groups to the silicate filler, which dramatically reduced the soluble fraction and bound pendent chain ends.

Additional evidence consistent with these results showed that the average molecular weight between crosslinks essentially decreased with the addition of both fillers, in particular when nanoparticles were used as reinforcements.<sup>14</sup> This was in agreement with the conclusions drawn by other authors upon the analysis of the influence of carbon black on the

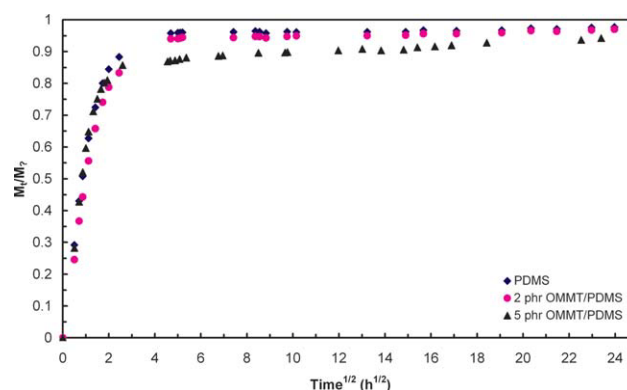


Figure 7 Swelling of pure PDMS and the OMMT/PDMS composites immersed in toluene  $M_t$  and  $M_\infty$  are the amount of solvent sorbed at time  $t$  and equilibrium, respectively. [Color figure can be viewed in the online issue, which is available at [www.interscience.wiley.com](http://www.interscience.wiley.com).]



average molecular mass of the elastomeric network. It was reported that the decrease in the average molecular weight between crosslinks was equivalent to an increase in the formation of polymer–filler couples and short bridging chains between the filler particles, which enlarge the extension of the filled network.<sup>21</sup>

## CONCLUSIONS

Our study of the preparation, characterization, and property testing of hydroxyl-terminated PDMS NCs containing commercial OMMT as a reinforcing agent led to the following conclusions:

Regarding the structure of the obtained NC samples, XRD analysis showed that within the experimental conditions of this study, at OMMT concentrations of 2 and 3.5 phr, exfoliation or delamination hybrids were formed, whereas at a concentration of 5 phr, the filler particles retained their integrity, and the system does not behave as an NC anymore.

The investigation of specimens by FTIR-ATR analysis did not reveal any particular chemical interactions between the organic part of the filler and the PDMS elastomer. Also, the initial temperature of thermal degradation and the temperature of the higher degradation rate did not display any significant changes, according to the results obtained from the TGA experiments, whereas an increase in the char residue was recorded for all of the tested samples, which was attributed to the efficient filler dispersion in the silicone matrix.

As to the effect of OMMT particles on the structure of the NCs, the data from DSC measurements indicated reductions in  $\Delta H_c$  and  $\chi_c$ , with the  $T_m$  remaining unaffected, which showed that the filler particles could not act as nucleating agents to further initiate crystallization of the system. On the other hand, DMA revealed an increase in  $T_g$  (for filler concentrations of 2 and 3.5 phr); this was probably the result of an increase in the network density caused by the filler nanoparticles. For an OMMT concentration of 5 phr,  $T_g$  returned to lower values because of the aforementioned characteristics of the composite. Finally, the nanolayer reinforcement led to improvements in the mechanical strength and stiffness of the examined samples.

The most important achievements of this study were probably the following:

1. The improvement in mechanical strength combined with the increased solvent resistance may provide additional evidence for the role of OMMT nanoparticles in the increase in the network density of the investigated silicone rubber NCs.
2. Taking into account the characteristics of the system and the parameter mixing procedure, we determined the range of concentrations where the nanofiller could produce intercalated or exfoliated structures.

## References

1. Siloxane Polymers; Clarson, S. J.; Semlyen, J. A., Eds.; PTR Prentice Hall: Upper Saddle River, NJ, 1993; Chapter 5.
2. Wang, J.; Chen, Y.; Jin, Q. *Macromol Chem Phys* 2005, 206, 2512.
3. Pinnavaia, T. J.; Beall, G. W. *Polymer Clay Nanocomposites* Wiley: Chichester, England, 2002; Chapter 5.
4. Burnside, S. D.; Giannelis, E. P. *Chem Mater* 1995, 7, 1597.
5. Wang, S.; Long, C.; Wang, X.; Li, Q.; Qi, Z. *J Appl Polym Sci* 1998, 69, 1557.
6. LeBaron, P. C.; Pinnavaia, T. J. *Chem Mater* 2001, 13, 3760.
7. Ma, J.; Xu, J.; Ren, J.-H.; Yu, Z.-Z.; Mai, Y.-W. *Polymer* 2003, 44, 4619.
8. Ma, J.; Yu, Z.-Z.; Kuan, H.-C.; Dasari, A.; Mai, Y.-W. *Macromol Rapid Commun* 2005, 26, 830.
9. Wang, J.; Chen, Y. *J Appl Polym Sci* 2008, 107, 2059.
10. Horsch, S.; Serhatkulu, G.; Gulari, E.; Kannan, R. M. *Polymer* 2006, 47, 7485.
11. Schmidt, D. F.; Clément, F.; Giannelis, E. P. *Adv Funct Mater* 2006, 16, 417.
12. Yang, L.; Hu, Y.; Lu, H.; Song, L. *J Appl Polym Sci* 2006, 99, 3275.
13. Wang, J.; Chen, Y.; Jin, Q. *High Perform Polym* 2006, 18, 325.
14. López-Manchado, M. A.; Arroyo, M.; Herrero, B.; Biagiotti, J. *J Appl Polym Sci* 2003, 89, 1.
15. López-Manchado, M. A.; Valentín, J. L.; Carretero, J.; Barroso, F.; Arroyo, M. *Eur Polym J* 2007, 43, 4143.
16. Schmidt, D. F.; Clément, F.; Giannelis, E. P. *Adv Funct Mater* 2006, 16, 417.
17. Kim, E.-S.; Kim, H.-S.; Jung, S.-H.; Yoon, J.-S. *J Appl Polym Sci* 2007, 103, 2782.
18. Burnside, S. D.; Giannelis, E. P. *J Polym Sci Part B: Polym Phys* 2000, 38, 1595.
19. Carretero-González, J.; Retsos, H.; Verdejo, R.; Toki, S.; Hsiao, B.; Giannelis, E. P.; López-Manchado, A. *Macromolecules* 2008, 41, 6763.
20. Takeuchi, H.; Cohen, C. *Macromolecules* 1999, 32, 6792.
21. Heinrich, G.; Vilgis, T. A. *Macromolecules* 1993, 26, 1109.